Available online at www.sciencedirect.com
SCIENCE DIRECT®
ELSEVIER
Nuclear Instruments and Methods in Physics Research A 522 (2004) 131–145
NUCLEAR INSTRUMENTS & METHODS IN PHYSICS RESEARCH Section A
www.elsevier.com/locate/nima

Status of design and construction of the Transition Radiation Tracker (TRT) for the ATLAS experiment at the LHC

T. Akesson[a], F. Anghinolfi[b], E. Arik[c], O.K. Baker[d], S. Baron[b], D. Benjamin[e], H. Bertelsen[f], V. Bondarenko[g], V. Bytchkov[h], J. Callahan[i], M. Capeáns[b], L. Cardiel-Sas[b], A. Catinaccio[b], S.A. Cetin[c], P. Cwetanski[b], M. Dam[f], H. Danielsson[b], F. Dittus[b], B. Dolgoshein[g], N. Dressnandt[j], C. Driouichi[a], W.L. Ebenstein[e], P. Eerola[a,*], P. Farthouat[b], O. Fedin[k], D. Froidevaux[b], P. Gagnon[i], Y. Grichkevitch[l], N. Grigalashvili[h], Z. Hajduk[m], P. Hansen[f], F. Kayumov[n,i], P.T. Keener[j], G. Kekelidze[h], A. Khristatchev[k], S. Konovalov[n], L. Koudine[k], S. Kovalenko[k], T. Kowalski[o], V.A. Kramarenko[l], K. Krüger[b], A. Laritchev[l], P. Lichard[b], F. Luehring[i], B. Lundberg[a], V. Maleev[k], I. Markina[g], K.W. McFarlane[d], V. Mialkovski[h], B. Mindur[o], V.A. Mitsou[f], S. Morozov[g], A. Munar[j], S. Muraviev[n], A. Nadtochy[k], F.M. Newcomer[j], H. Ogren[i], S.H. Oh[e], S. Oleshko[k], J. Olszowska[m], S. Passmore[b], S. Patritchev[k], V. Peshekhonov[h], R. Petti[b], M. Price[b], C. Rembser[b], O. Rohne[j], A. Romaniouk[h,g], D.R. Rust[i], Yu. Ryabov[k], V. Ryjov[h,j], V. Schegelsky[k], D. Seliverstov[k], T. Shin[d], A. Shmeleva[n], S. Smirnov[g], V. Sosnovtsev[g], V. Soutchkov[g], E. Spiridenkov[k], R. Szczygiel[m], V. Tikhomirov[n], R. Van Berg[j], V.I. Vassilakopoulos[d], L. Vassilieva[n], C. Wang[e], H.H. Williams[j], A. Zalite[k]

[a] *Fysiska Institutionen, Lunds Universitet, Lund, Sweden*
[b] *European Laboratory for Particle Physics (CERN), Geneva, Switzerland*
[c] *Department of Physics, Bogazici University, Istanbul, Turkey*
[d] *Hampton University, Hampton, VA, USA*
[e] *Physics Department, Duke University, Durham, NA, USA*
[f] *Niels Bohr Institute, University of Copenhagen, Copenhagen, Denmark*
[g] *Moscow Engineering and Physics Institute, Moscow, Russia*
[h] *Joint Institute of Nuclear Research, Dubna, Russia*
[i] *Department of Physics, Indiana University, Bloomington, Indiana, USA*
[j] *Department of Physics and Astronomy, University of Pennsylvania, Philadelphia, PA, USA*
[k] *Petersburg Nuclear Physics Institute, Gatchina, St. Petersburg, Russia*
[l] *Moscow State University, Institute of Nuclear Physics, Moscow, Russia*

*Corresponding author. Department of Elementary Particle Physics, Lund University, P.O. Box 118, Lund 22100, Sweden Tel.: +46-46-222-7695; fax: +46-46-222-3601.
E-mail address: paula.eerola@quark.lu.se (P. Eerola).

0168-9002/$ - see front matter
doi:10.1016/j.nima.2004.01.033

[m] Henryk Niewodniczanski Institute of Nuclear Physics, Cracow, Poland
[n] P.N. Lebedev Institute of Physics, Moscow, Russia
[o] Faculty of Physics and Nuclear Techniques of the Academy of Mining and Metallurgy, Cracow, Poland

Abstract

The ATLAS Inner Detector consists of three sub-systems, the Pixel Detector at the innermost radius, the Semi-Conductor Tracker at intermediate radii, and the Transition Radiation Tracker (TRT) at the outermost radius in front of the electromagnetic calorimeter. The TRT provides a combination of continuous tracking with many projective measurements based on individual drift-tubes (or straws) and of electron identification based on radiator fibres or foils interleaved between the straws themselves. This paper describes the current status of design and construction of the various components of the TRT: the assembly of the barrel modules has recently been completed, that of the end-cap wheels is well underway, and the on-detector front-end electronics is in production. The detector modules and front-end electronics boards will be integrated together over the next year, the barrel and end-cap TRT parts will be assembled and tested with their SCT counterparts during 2005 and installation and commissioning in the ATLAS pit will take place at the end of 2005 and the beginning of 2006.

PACS: 29.40.Cs

Keywords: Transition radiation; LHC; Straw tracker; Read-out electronics

1. Introduction

The Transition Radiation Tracker (TRT) is one of the three sub-systems of the ATLAS Inner Detector [1], designed to operate in a 2 T solenoidal magnetic field at the design luminosity (10^{34} cm^{-2} s^{-1}) of the CERN LHC. As shown in Fig. 1, the TRT provides a combination of continuous tracking with many projective measurements based on individual drift-tubes (or straws) and of electron identification based on radiator fibres or foils interleaved between the straws themselves. With this choice of straw geometry, all charged particle tracks with transverse momentum $p_T > 0.5$ GeV and with pseudo-rapidity $|\eta| < 2.5$ cross about 35 straws (except for the barrel/end-cap transition region).

The straw diameter was chosen to be 4 mm as a reasonable compromise between speed of response, number of ionisation clusters, and mechanical and operational stability. Each straw is reinforced along its length with four sets of thin C-fibre filaments, which provides it with stability in terms of thermal and humidity variations. The straw anodes are 30 μm diameter gold-plated tungsten wires at ground potential and the straw cathodes, made from a coated polyimide film, are typically operated at a high voltage of 1530 V, corresponding to a gas gain of 2.5×10^4 for the chosen gas mixture containing 70% xenon, 27% CO_2 and 3% O_2.

At LHC rates, significant heat is generated in the straws as the positive ions created by the ionising particles drift to the cathode. The heat dissipation is directly proportional to the straw counting rate and is estimated to be 10–20 mW per straw at the LHC design luminosity. Considering the basic requirements on straw operation stability and gas-gain uniformity, the temperature gradient along each straw should not exceed 10°C. To meet this specification and to evacuate the heat, a flow of CO_2 gas along the straws is used in the end-cap wheels; in contrast, fluorinert liquid, used to cool the barrel front-end electronics, maintains the barrel-module shells at an approximately constant temperature. The flow of CO_2 also evacuates any xenon gas which would leak out of the straws, thereby potentially polluting the radiator space.

Because of their different geometries, the barrel modules and end-cap wheels are structurally

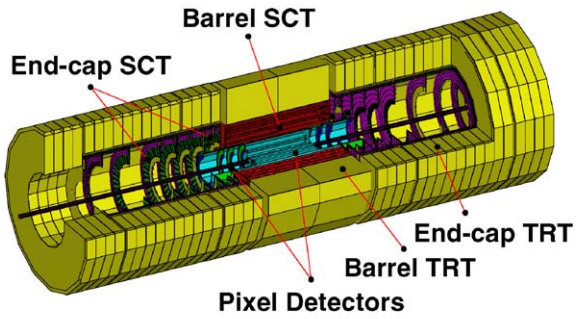

Fig. 1. Perspective view of the ATLAS Inner Detector with its three sub-systems: the Pixel Detector at the innermost radii, the Semi-Conductor Tracker (SCT) at the intermediate radii, and the TRT at the outermost radii. The barrel TRT contains 52,544 axial straws of 144 cm length and each end-cap TRT contains 159,744 straws of 37–53 cm length.

different, but nevertheless follow the same tight requirements in terms of rigidity, dimensional stability, minimum amount of material and other features characteristic of any tracking system in a collider experiment. The assembly procedures have been optimised for fast and reliable mass production. The appropriate modularity has been used throughout the detector to simplify these assembly procedures and to minimise at every stage the number of straws affected by any failure in the overall system. The quality-control procedures and specifications to be met during the course of production are an integral part of the assembly process. A powerful production database and user-friendly web interface support the storage of parts, the input quality-control data for all components, as well as the identification and storage of all test results obtained during the assembly itself.

2. Design and construction of the barrel TRT modules

2.1. Overview

The barrel TRT consists of three cylindrical rings, each containing 32 identical and independent modules of 144 cm length, as shown in Fig. 2. To reduce the straw occupancy, the anode wires

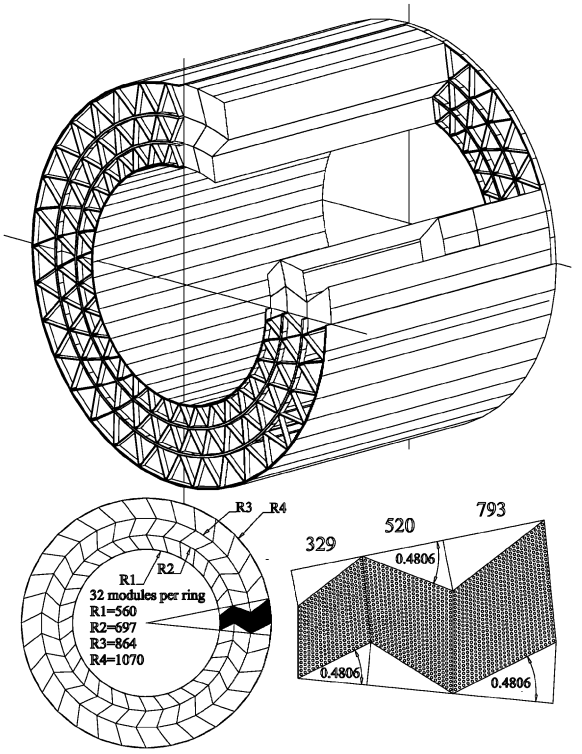

Fig. 2. Layout of the barrel TRT with its three concentric rings of 32 identical modules each. Also shown at one end is the barrel support structure, which will hold all the modules in place within the ATLAS barrel cryostat.

are electrically separated in the middle by a glass wire-joint and are read out from both ends. The smallest modules (type-1) contain 329 axial straws positioned in 19 layers at the innermost radius; the first nine radial layers are equipped with two wire-joints per wire, and are therefore active only over the last 31 cm on each end. This further reduces their occupancy, while maximising the number of crossed straws for tracks traversing the barrel/end-cap transition region. The type-2 modules contain 520 axial straws positioned in 24 layers at an intermediate radius, and the type-3 modules contain 793 axial straws positioned in 30 layers at the outermost radius.

The modular design approach reduces risk during assembly, enables distributed production at several assembly sites and speeds up the final assembly process because each module can be tested independently. As can be seen from Fig. 2,

all three types of modules have the same shape even though they are different in size. The shape and arrangement of the modules are designed to minimise the probability of losing tracks in the cracks between modules. Table 1 shows the main parameters relevant to each module type. The average straw spacing is 6.8 mm and the straw azimuthal positions are staggered between consecutive layers, leading to a uniform geometry well optimised for continuous tracking. A typical track will cross 36 out of the 73 layers of straws. The space between straws is filled with 15 μm diameter polypropylene/polyethylene fibre radiator, which results in about 7 transition-radiation hits observed on average for a 20 GeV p_T electron.

Table 1
Key parameters defining the three different types of barrel modules

	Type 1	Type 2	Type 3
Number of straws per module	329	520	793
Number of straw layers per module	19	24	30
Module inner radius (mm)	560	697	864
Module outer radius (mm)	695	862	1070

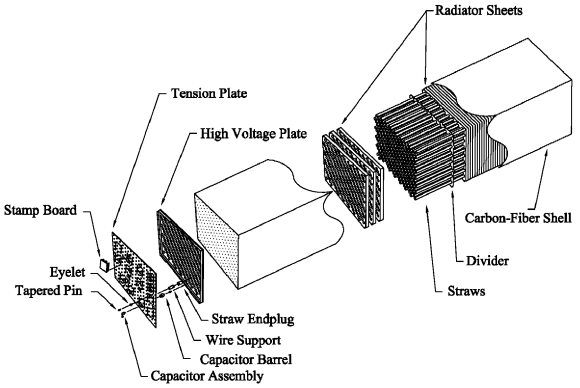

Fig. 3. Exploded view of barrel module, showing the various mechanical components within the module itself and at one of its ends (see text).

2.2. Module design

Inside a module, the straws are embedded in radiator sheets and supported by dividers every 25 cm along the module length. At the ends of the module, the straws are supported by and conductively glued to high-voltage plates for fixation and high-voltage connection. A carbon-fibre shell, glued to the high-voltage plates and dividers along with the carbon-fibre-reinforced straws, provides the required mechanical rigidity and stability to the module. Figs. 3 and 4 show an exploded view of a module and some of the details of the module end. A printed-circuit board, called tension plate, is glued to the high-voltage plate and holds the tension of the wires and interfaces the module to the read-out electronics. Metallic eyelets and tapered pins are used to fix the wires to the tension plate (the typical tension applied to each wire is about 60 g). The tension plate is a double-sided printed-circuit board with traces between the eyelets and sockets, which receive the front-end electronics boards (see Section 4.3.3).

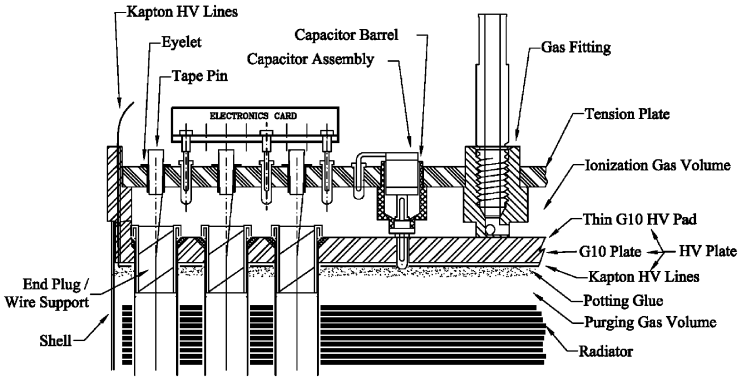

Fig. 4. Detailed view of one end of a barrel module (see text).

The space between the tension plate and the high-voltage plate is a buffer, through which ionisation gas is fed into the individual straws. Within the shell, the space outside the straws, which is almost entirely filled by the radiator, is normally purged with CO_2 during operation to clean out any leakage of Xe gas. As shown in Fig. 4, polyimide foils carrying the high-voltage lines follow the sides of the high-voltage plate to minimise the disruption to the leak-tightness of the Xe-containing gas volume. From the back-side of the high-voltage plate, the high-voltage lines are brought to the front through sockets that also connect to the bypass capacitors. Each bypass capacitor serves as the AC ground return for the signals from eight straws, which share the same high-voltage line.

2.3. Module assembly

The assembly of the barrel modules is performed at three assembly sites in the US. The module-assembly process can be roughly described as the following sequence of steps: component preparation, mechanical assembly, stringing of the anode wires and final tests resulting in the establishment of a "passport" for each module.

2.3.1. Component preparation

Each component, when received from a manufacturer or produced in-house, has to be checked for conformance and cleaned before use. Some of the components go through several stages of assembly before going into a module (straws, wires equipped with glass wire-joints, high-voltage plates, tension plates). In these cases, quality control is performed after each salient stage of assembly.

2.3.2. Mechanical assembly

The assembly of a module starts with an alignment check of its structural components: the two high-voltage plates, the five dividers and the shell. These components determine the straightness of straws inside a module. The components are assembled in an alignment frame, which holds them in place until structural assembly is complete. Nine reference straws are then inserted and surveyed for their straightness using a laser system. The components are accepted if the straightness of these reference straws is measured to be within ± 180 μm.

The high-voltage plates and dividers are then removed and reinstalled with packs of radiators. Once the high-voltage plates have been fixed to the shell, the straws are inserted with care: an insertion "bullet" made from a Mylar sleeve and a Delrin rod, as shown in Fig. 5, is used to protect the end of the straws and guide them through the radiators. To avoid pushing a radiator pack towards one side of the module, the straws are inserted in alternating directions in a sequence spiraling outward from the centre. After the straws are inserted, a high-voltage test cycles 2500 V through each group of eight straws while the rest of the straws are kept at ground potential. The straws are then conductively glued to the high-voltage plate with end-plug wire supports (see Fig. 4).

The high-voltage test is repeated after each side is glued. After the conductive glue has cured, the straw ends are further sealed to the face of the high-voltage plate with low-viscosity epoxy to improve the mechanical strength and the gas tightness. In the meantime, the high-voltage plates and dividers are also glued to the shell. At this point, the module is structurally complete and removed from the alignment frame. With the module standing vertically, the back sides of the high-voltage plates are potted with low-viscosity

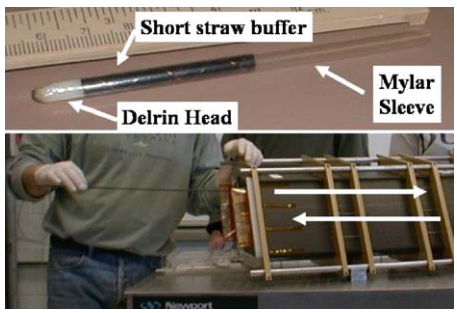

Fig. 5. Photograph of straw insertion bullet (top) and of the insertion of a straw (bottom). The arrows indicate the insertion sequence.

epoxy to ensure a gas seal. At the end of this mechanical assembly, the module is tested for gas tightness (leak rate below 1 mbar/bar/min) and high-voltage stability (2500 V for each straw group), and it is then sent to a stringing station.

2.3.3. Anode-wire stringing

The stringing of the anode wires for the barrel TRT modules has been a particularly delicate and time-consuming operation, because of the glass wire-joints and of the three helical locator pieces (one at each end and one in the middle of the straw), through which the wire and its glass wire-joint(s) must pass without getting stuck in the process.

The anode wire is inserted and the glass wire-joint (see Fig. 6) is positioned correctly inside the straw through a sequence of operations. Before stringing, the anode wire is placed under tension and an anchor is attached at correct distance from the wire-joint. A Cu–Be lead wire of 50 μm diameter is blown through the straw, tied to the anode wire, and used to pull it into the straw, through eyelets in the tension plate. The anchor stops the insertion of the anode wire, positioning the wire-joint at the desired location. The anode wire is then tensioned and clamped with tapered pins inserted in the eyelets. Because of the flexibility of the tension plate, stringing is performed sequentially from the edges towards the centre, to minimise tension losses possibly arising due to tension-plate warping. The mechanical tension and the high-voltage stability of the anode wires are tested during the stringing process. Any wire with a problem is re-worked until it passes the requirements. After stringing, the tapered pins and eyelets are sealed for gas tightness and the module is considered complete (as a mechanical object).

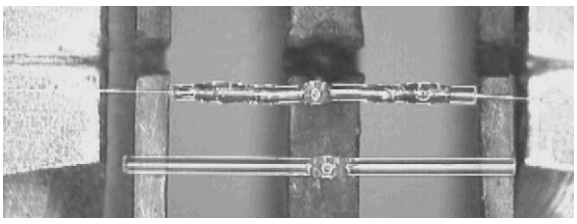

Fig. 6. Photographs of a glass tube melted in its centre and used to make the wire-joints (bottom) and of a finished glass wire-joint (top).

2.4. Module testing and passport

Before modules are shipped to CERN from the assembly sites, a series of tests is done to ensure their quality and to prepare the first part of the so-called module passport. These tests include:

- Dimension checks and a module-mounting test to make sure that the module can be freely mounted into the barrel support structure (see Fig. 2).
- Gas-tightness measurements in the ionisation volume and in the purging volume.
- Measurements of wire tensions and high-voltage stability.
- Measurements with an X-ray source, to make sure every wire segment is functional or flagged in the module passport, if not.
- Mapping of the whole module with an X-ray tube [2] to measure the gas-gain variation along each wire segment and to note any anomalies for possible re-work at a later stage.

The module passport contains directly all the important parameters characterising it, and also includes links to the data from the various measurements done before and after assembly. The gas-gain uniformity along a wire segment is a critical element for stable operation over many years at the LHC. More than 99% of all straws are found to be well within the required specifications, namely a gas-gain variation below 10%, corresponding to a wire offset below 400 μm. Fig. 7 shows the results from the X-ray gain mapping for two examples of straws with a gas-gain variation above 10%. The first straw displays a behaviour typical of a wire not smoothly passing through the central wire support: this can be repaired by restringing the wire. The second straw is a more worrisome case, since it appears to be really bent between the dividers: this straw will have to be disabled by removing the wire completely.

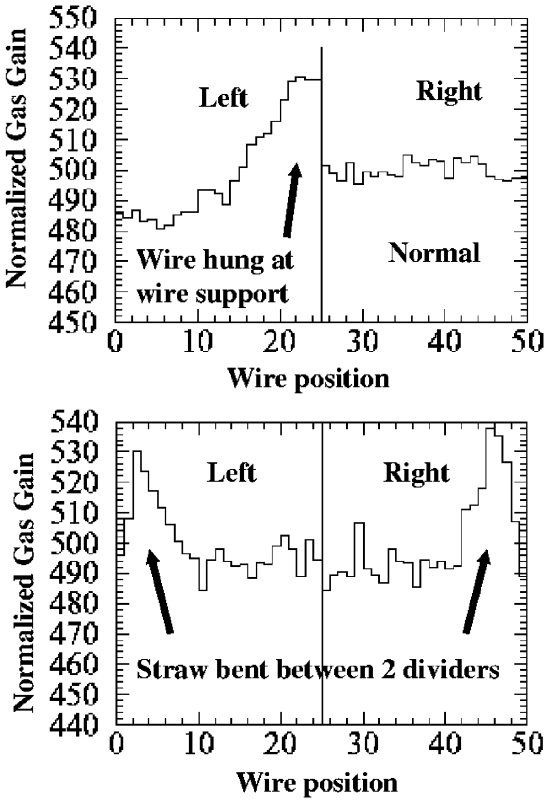

Fig. 7. Results from the X-ray gain mapping for two abnormal straws. One straw (top) has its left-hand wire segment hung at the central wire support. The second straw (bottom) is bent between two dividers.

with 15 μm thick polypropylene radiator foils. The distance between straws in the azimuthal plane varies between 5.2 mm at the inner radius of 640–8.4 mm at the outer radius of 1010 mm. The second type of wheels (type B: eight 8-plane wheels per side at $1719 < z < 2725$ mm) is identical to the type-A wheels except for the spacing between successive straw layers which is increased to 15 mm. The free space between successive layers is thus increased from 4 to 11 mm and it is filled with a larger number of radiator foils.

Finally, the third type of wheels (type C: eight wheels per side at $2818 < z < 3363$ mm) contains 4608 straws positioned in eight successive layers spaced by 8 mm along z (as for the type-A wheels). Each layer, however, contains only 576 straws in the azimuthal plane, a smaller number than for the type-A/B wheels. This is because the type-C straws are longer by 14 cm than their type-A/B counterparts with an inner radius at 480 mm to extend the η-coverage of the TRT. The construction of the type-C wheels has been staged and they will not be discussed further here.

The end-cap TRT therefore comprises a total of 319,488 straws with a fairly uniform occupancy. A typical track will cross between 32 and 45 straws and a total of between 10 and 15 high-threshold hits from transition radiation will be observed for a high-p_T electron.

3. Design and construction of the end-cap TRT wheels

3.1. Overview

As illustrated in Fig. 1, each of the two end-cap TRT parts consists of three sets of identical and independent wheels, called 8-plane wheels, because they contain eight planes of radially oriented straws. The first type of wheels (type A: twelve 8-plane wheels per side at $827 < z < 1715$ mm) contains 6244 straws positioned in eight successive layers spaced by 8 mm along z; each layer contains 768 straws in the azimuthal plane and the free space of 4 mm between successive layers is filled

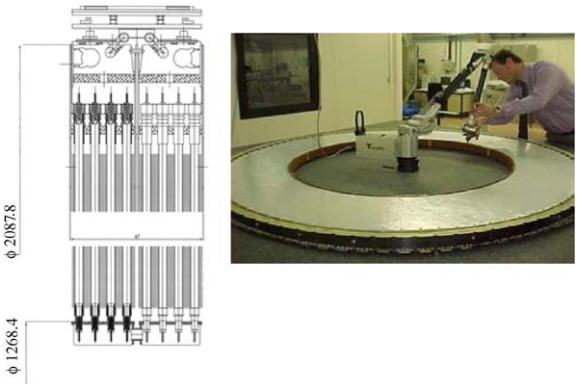

Fig. 8. Drawing of the detailed layout of a type-A 8-plane wheel (left) and photograph of one of the wheels assembled in Russia and under tests at CERN.

3.2. Wheel design

Fig. 8 shows the layout of a type-A 8-plane wheel and a photograph of one of the wheels assembled in Russia after it has been delivered to CERN. The 8-plane wheel is in fact an assembly of two back-to-back 4-plane wheels, which are the basic assembly unit for the detector.

The straws are inserted and glued into precisely drilled holes in an inner and an outer C-fibre ring, which serve as support structures for the straws. The successive layers of straws are positioned such that a straw in a given layer is angularly displaced with respect to its partner in the previous layer by only $\frac{3}{8}$ of the azimuthal spacing between straws in the same layer. This ensures optimal uniformity in the number of straws crossed by particles as a function of azimuth.

For the high-voltage and signal connection a flex-rigid printed-circuit board is used (see Fig. 9). One of the flexible layers of the circuit, made of polyimide, contains holes with inward-pointing petals. To provide a reliable high-voltage connection to the straw cathode, these petals are forced into contact with the inner straw wall through the insertion of a plastic high-voltage plug through the petals into the straw.

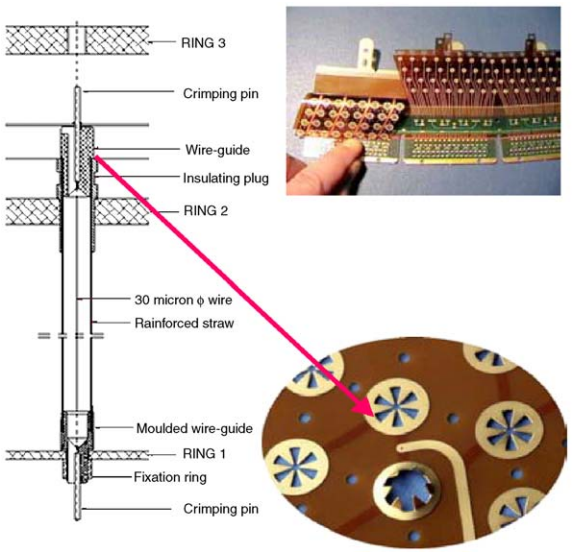

Fig. 9. Drawing of end-cap straw (left) and of the various components used to position it and connect it to high-voltage and to the front-end electronics (see text). Also shown (top right) is a photograph of the flex-rigid printed-circuit board used to bring high voltage to the straws and collect the signal from the anode wire. Specially etched metallic petals (bottom right) are used to provide the connections needed.

The signal connection is done in an analogous way using a second flexible layer, also containing holes with metallic petals. Custom-designed copper crimp-tubes are used on both ends of the straw to position and fix the wire. The flex-rigid printed-circuit board transmits the signal collected on the anode wire to the front-end electronics boards (see Section 4.3.3) through three connectors, each corresponding to 32 channels.

A third C-fibre ring at the outer radius is glued to the rigid part of the flex-rigid printed-circuit board described above and to a simpler glass-fibre board on the opposite side of the 4-plane wheel, thereby providing a sturdy box-like support structure together with the outer C-fibre ring at a slightly lower radius, used to fix the straws themselves. This box-like structure also serves as an outer gas manifold for the 4-plane wheel. The gas actually flows into one of the two 4-plane wheels, assembled together as an 8-plane wheel, through this outer gas manifold, along the straws, into an inner gas manifold, made of reinforced polyimide material, and through eight plastic connecting elements into the second 4-plane wheel, where it traverses the straws in the opposite direction and is collected in its outer gas manifold.

The whole 8-plane wheel is covered with a thin metal-clad polyimide membrane on each side and at the inner radius, which provides a signal-return path from the inner radius of the straws to the outer radius, where the electronics ground is defined. Additional membranes are used to provide the required path for the CO_2 cooling gas, which enters each wheel at its inner radius, flows out along the straws and radiator foils, is collected and cooled in a heat exchanger located at the outer radius between groups of one or two 8-plane wheels, and then flows down to the next wheel. The wheels are held together as a stack through a set of axial metallic tie-rods and each stack of wheels is supported on rails fixed to the ATLAS barrel cryostat.

3.3. Wheel assembly

The assembly of the end-cap wheels is performed at two assembly sites in Russia. The wheel-assembly process can be roughly described as the following sequence of steps: component preparation, mechanical assembly, stringing of the anode wires and final tests, resulting in the establishment of a "passport" for each wheel.

3.3.1. Procurement and preparation of components

The status of the procurement of the major components for the type-A/B end-cap wheels is shown in Table 2. At this stage of the project, all components are technically well in hand and not on the critical path with one major exception: the flex-rigid printed-circuit boards, which still require further technical work to obtain reliable and stable quality of manufacturing and which currently drive the schedule of the assembly sites in Russia.

Each component, when received from a manufacturer or produced in-house, has to be checked for conformance and cleaned before use. Some of the components go through several stages of assembly before going into a module (straws, flex-rigid printed-circuit boards, inner gas manifolds). In these cases, quality control is performed after each salient stage of assembly.

3.3.2. Mechanical assembly

In contrast to the barrel straws, the end-cap straws are not supported along their length and particular care has to be taken during their insertion into the holes in the C-fibre rings to preserve their straightness, which is required to be better than 200 μm after the completion of the straw preparation itself. Each straw is therefore inspected after insertion, both visually and using optical tools, and problematic straws are replaced before gluing. The complete operation of straw insertion, inspection and quality-control measurements (dimensions, gas tightness of the mechanical structure) requires about three weeks per 4-plane wheel. Currently, 70% of the mechanical structures have been successfully assembled.

Table 2
Status of component procurement for the type-A/B end-cap wheels

Component type	Availability (%)
Straws prepared for assembly	100
Radiators	100
C-fibre support rings	88
Flex-rigid printed-circuit boards	20
Plastic high-voltage plugs	100
Anode wire	90
Crimp-tubes	40
Other components	80

3.3.3. Anode-wire stringing

The next step in the assembly process is the gluing of the flex-rigid printed-circuit boards to the outer ring holding the straws, followed by the insertion of the plastic high-voltage plugs and a first high-voltage test of the wheel. This is followed by the stringing of the anode wires, the most time-consuming operation of the whole assembly process, but more straightforward than in the case of the barrel modules because of the shorter length of the end-cap straws and of the more standard crimping technique used.

Approximately, 50,000 end-cap wires have been strung to-date and in routine operation less than 1% of the wires have to be restrung. The tension of the wires is measured during the stringing process itself and a final global wire-tension measurement is done before moving to the next major assembly step, which is the gluing of the third and outermost C-fibre ring to the flex-rigid printed circuit boards. After this operation, wire-stringing becomes a major re-work operation. Such re-work has unfortunately happened in a few cases, because of damages to the flex-rigid printed-circuit boards.

The final assembly steps are simpler but numerous and are all related to the closure of the 4-plane wheel at its inner and outer radii, followed by the assembly of the 8-plane wheel itself.

3.4. Wheel testing and passport

In addition to the quality control and tests performed during assembly, all completed 8-plane wheels are submitted to a set of measurements before they are packaged to be sent to CERN and again upon arrival at CERN. These measurements follow similar procedures and tooling to those

Table 3
List of acceptance tests with their specifications and typical values obtained for the end-cap wheels at the assembly sites and at CERN after transport

Acceptance test	Specification	Typical values
Gas tightness (mbar/min/bar)	1.0	0.15
HV current (nA, no wires)	50 at 2500 V	<10
Wire tension T (g)	$55<T<80$	70
HV current (nA, with wires)	50 at 1800 V	<10
Gas tightness (mbar/min/bar)	1	0.05
HV current (nA, Ar/CO_2)	50 at 1800 V	10
Gas-gain variation	All channels with <400 μm wire offset	$<0.1\%$ of all channels

used during assembly. For the final evaluation of each wheel, the critical points and specifications summarised in Table 3 are considered.

All the wheel characteristics are recorded in the production database and all the measurements are compared with the values obtained during production. The final information is included in the electronic passport of each wheel. In contrast to the barrel module case, wires found to be out of specifications in the end-cap wheels are neutralised, i.e. disconnected from their high-voltage group by unsoldering the protection resistor, since the design does not permit direct restringing of wires.

The verification of the straw straightness, or wire offset with respect to its nominal position within the straw, is the most critical test of the full set of acceptance criteria. For a wire offset of more than 400 μm, the local increase of electric field substantially modifies the gas gain. Under such conditions, the rate of discharges and large-amplitude signals increases significantly, making the straw very unstable under standard LHC running conditions. Therefore, such wires are disconnected from the high-voltage supply, as described above.

The verification is performed by installing the 8-plane wheel under test in a vertical position in an automated set-up equipped with an array of ^{55}Fe sources. These ^{55}Fe sources are mounted on arms placed at six different radii on a star-shaped support. Through an automatic rotation of the arms, the signal amplitude, obtained in a 70% Ar-30% CO_2 gas mixture, is read out at six points along the full length of each individual straw. For a perfectly straight straw with an anode wire exactly centered at the straw ends, the amplitude of the signal should be very uniform along the full length of the straw. The actual overall wire offset will arise from several different sources, e.g. the precision and play in the straw plastic end-pieces, the crimp tubes, etc. However, the main cause for wire offset is a bent or non-circular straw.

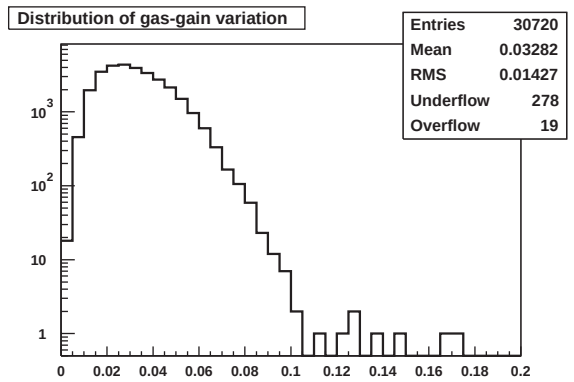

Fig. 10. For all straws of the first five assembled 8-plane end-cap wheels, distribution of the relative variation of gas-gain along each straw. The entries in the underflow bin correspond to dead or unstable channels, which are still under investigation.

The goal is to have 95% of the straws measured with an eccentricity below 300 μm, which corresponds to a relative variation of about 5.5% in signal amplitude for the chosen gas. All wire offsets should hopefully stay below 400 μm, corresponding to less than 10% gas-gain variation. Fig. 10 shows the distribution of the relative variation in gas gain for the first five 8-plane

wheels assembled in Russia and delivered to CERN, corresponding to a total of 30,720 channels. The average is close to 3% with an r.m.s. spread of 1.4%, demonstrating the excellent quality of the assembled wheels. Less than 1% of all channels are dead or unstable; the main contribution to these arises from damages to the flex-rigid printed-circuit boards and is still under investigation. Less than 0.1% of the straws display a wire offset above 400 μm and will have to be neutralised. The reproducibility of the gas-gain variation measurements between the production sites and CERN, as well as between repeated runs, is better than 1%, thanks in particular to a careful control and monitoring of environmental conditions.

4. The TRT read-out system

4.1. Design challenges for the TRT read-out

The TRT on-detector front-end electronics and off-detector read-out (or back-end) system are designed to exploit the full performance potential of the TRT detector within the harsh experimental environment of the ATLAS experiment at the LHC.

At the highest luminosity, each bunch crossing contains on average 23 primary proton–proton collisions, leading to TRT straw hit probabilities as high as 40% for the innermost barrel straws and the longest end-cap straws. Since the maximum electron drift-time of 48 ns with the newly adopted $Xe/CO_2/O_2$ gas mixture is almost twice as long as the time between bunches, overlapping hits clearly cannot be avoided. To minimise the performance-degradation associated with the large hit probability, the analogue signal processing must provide accurate ion-tail cancellation and rapid return-to-baseline for a wide dynamic range of signals.

Given the very high LHC bunch-crossing frequency of 40 MHz, all ATLAS detectors need to store their data for the 2.5 μs duration of the level-1 trigger latency. Furthermore, detector read-out should not induce dead-time even as the level-1 accept rate approaches its ultimate goal of 100 kHz; this requirement not only translates into a simple bandwidth requirement for the front-end and read-out links, but also has implications for the depth of the on-detector data derandomisation buffers and for the data-compression requirements of the back-end system.

The spatial and physical constraints of any on-detector electronics for tracking detectors near the beams normally call for a high-channel density and minimum power dissipation. The integration of high-speed, sensitive analogue amplifiers with digital circuits clocked at 40 MHz requires solutions to complex problems in the domain of electromagnetic compatibility (EMC). The TRT front-end electronics are in addition required to operate under the harsh LHC radiation load for 10 years, and are therefore expected to survive a total ionising dose of up to 5 Mrad and a total neutron fluence of up to 2×10^{14} n/cm^2. Because of the expected high density of particles, the digital

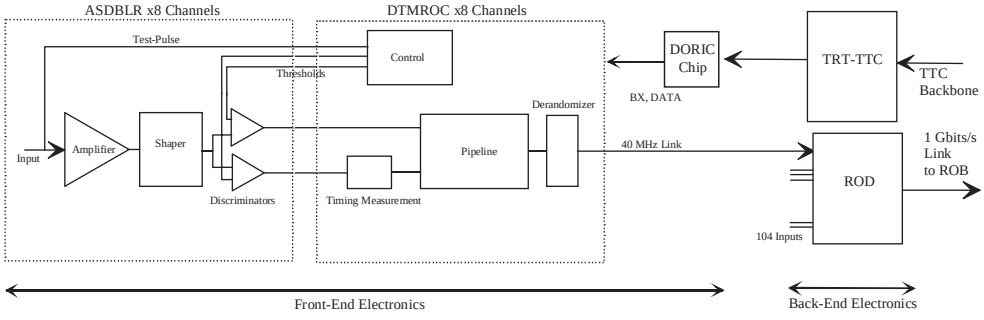

Fig. 11. Architecture of the TRT read-out system from on-detector electronics to off-detector read-out drivers (see text).

circuitry must be as resistant as possible to single-event upsets (SEU), and the overall read-out system must be tolerant to a non-zero residual rate of such events.

4.2. System architecture and characteristics

Fig. 11 shows the overall architecture of the TRT read-out system, which comprises a total of 424,576 electronics channels. The recording of drift-time and transition-radiation hits is performed by means of dual discriminators; at the nominal gas gain of 2.5×10^4, the typical operating thresholds are 2 fC (0.2 keV) and 60 fC (6 keV), respectively.

The analogue signal processing and threshold discrimination, as well as the subsequent time digitisation and data pipe-lining, are implemented in the on-detector electronics. A chip-set of one digital (DTMROC) and two analogue (ASDBLR) chips handles 16 channels and is a self-contained unit in terms of threshold setting and data pipe-lining. Events tagged by the ATLAS level-1 trigger are read out through derandomising buffers with one 40 Mbit twisted-pair LVDS-link per 16 front-end channels.

In order to optimise data access for the level-2 trigger processors, the segmentation of the TRT read-out system follows $\frac{1}{32}(11.25^\circ)$ azimuthal slices of the detector. Each end of such a barrel slice has 104 digital read-out chips, feeding their read-out links into one off-detector VME-based module, called read-out driver (ROD). The 240 read-out chips of each corresponding end-cap azimuthal slice (for the initial detector) connect to two RODs. The complete read-out system for the initial detector thus comprises 192 RODs (a total of 32 additional RODs will be needed to read out the staged end-cap wheels covering the edge of the TRT pseudo-rapidity range (see Section 3.1)). The clock-distribution domains are orthogonal to the read-out segmentation and are defined as 8-plane wheels in the end-cap TRT and layers at approximately constant radius in the barrel TRT. The drift-time t_0 can be set independently in 1 ns steps for each domain, a functionality provided by the TRT interface to the ATLAS Trigger, Timing and Control system (TRT-TTC).

4.3. On-detector electronics

The TRT front-end chip-set was originally conceived as being fully implemented in a radiation-hard 0.8 μm BiCMOS process (DMILL), optionally integrating one digital and two analogue chips into a single-die 16-channel unit. Yield considerations however led to abandoning the idea of full analogue/digital integration, and as very reasonably priced sub-micron CMOS processes became available, the digital chip was migrated to a 0.25 μm CMOS technology (DSM). The analogue chip requires bipolar transistors and has therefore been produced in the DMILL technology.

4.3.1. Analogue front-end chips

The TRT analogue shaper discriminator baseline restorer (ASDBLR) chip integrates 8 identical channels on a $3.3 \times 3.6\ \mathrm{mm}^2$ die for a 340 μm channel pitch. The power consumption of 40 mW/channel is well within the foreseen power budget.

Each channel features a dual preamplifier; the active input is connected to the anode wire, while a dummy input is available for pick-up cancellation. The intrinsic noise is 0.3 fC and the dynamic range exceeds 100 fC. The signal-processing stages provide a 7–8 ns shaping time and precise ion-tail cancellation, programmable for the baseline Xe-mixture or a faster Ar-based gas. The baseline-restorer network ensures a fast return to baseline, in the range of 25–50 ns, depending on the signal amplitude. The discriminator outputs are encoded into differential current-mode ternary drivers.

The ASDBLR has been thoroughly studied in test beam and is found to perform very well, as reported elsewhere in these proceedings [3,4]. The radiation hardness has been verified up to a total ionising dose of 7 Mrad and no significant change of performance has been observed. In terms of non-ionising energy losses (NIEL), samples have been exposed to $7 \times 10^{14}\ \mathrm{n/cm}^2$, resulting in a gain reduction of 50%, but otherwise fully functional chips. These doses correspond to 10 years of operation at the LHC and include a safety factor of three.

The DMILL process has however shown an unexpectedly large loss of transistor beta due to

thermal neutrons, because the damage per thermal neutron turns out to be approximately three times larger than the nominal damage due to 1 MeV neutrons. Approximately half of the neutron fluence in the ATLAS Inner Detector is expected to arise from thermal neutrons, and the safety factor of three quoted above is therefore reduced to 1.5. If reduced amplifier gain turns out to affect the performance of the detector, some recovery might be achieved by increasing the operating voltage.

All ASDBLR wafers have been delivered by the manufacturer, and are currently being packaged in custom fine-pitch ball-grid array technology (fpBGA). Preliminary yield measurements from wafer-level testing are very encouraging, and the final results await the completion of the testing of the full set of production chips.

4.3.2. Digital front-end chips

As explained above, the TRT drift-time measurement read-out chip (DTMROC) was originally implemented in DMILL, then redesigned in a 0.25 μm CMOS technology, as a result of a concentrated engineering effort. The full set of chips has now been manufactured and packaged in fpBGA technology, using the mask-set of the first and only engineering run, with excellent production yield. Samples have passed stringent tests of radiation hardness and sensitivity to single-event upsets (SEU).

The DTMROC front-end samples the status of the drift-time discriminators eight times per bunch-crossing, performing time measurements with a 3.125 ns bin size (corresponding to a 1 ns resolution). The sampling clocks are generated by means of local delay-lock-loops (DLL), synchronised to the external 40 MHz system clock. The status of the transition-radiation discriminator is latched as well, and, as a result, the DTMROC front-end produces a total of 9 data bits per bunch-crossing and per channel.

The drift-time and transition-radiation bits are fed into a synchronous pipeline implemented using two banks of dual-port RAM. The effective depth of the pipeline is programmable, to a maximum of 255 cycles or 6.3 μs. Upon reception of a level-1 accept, data from three consecutive bunch-crossings are queued for read-out through the derandomising buffer, implemented again as dual-port RAM with a maximum depth of 42 events, guaranteeing virtually no induced dead-time at the design level-1 trigger rate of 100 kHz.

The DTMROC includes four programmable digital-to-analogue converter outputs intended to set the drift-time and transition-radiation thresholds for the two partner ASDBLR chips. Featuring also a number of test, diagnostics, and temperature- and voltage-monitoring functions, the chip-set constitutes a self-contained unit with respect to control and data taking.

4.3.3. On-detector electronics integration

The on-detector electronics for the end-cap wheels have moderate channel density in the transverse plane, since they are located at the outer radius. They also are provided with a reasonable amount of space in the radial direction and a uniform geometry, which allows a simple and compact implementation. The analogue and digital chips are placed on physically different printed-circuit boards; there is one type of analogue board for each wheel-type, and one type of digital board common to all wheels. Groups of three analogue boards with a digital board are stacked up on the outer surface of the end-cap wheels, outside the cooling structure; one such 192-channel unit is shown in Fig. 12. This design ensures high immunity to clock pick-up. The end-cap boards have been submitted to extensive medium-scale test-beam and system test measurements [5–7], and are basically ready for mass-production. A total of 1280 3 + 1-units are needed to equip the A- and B-parts of the TRT.

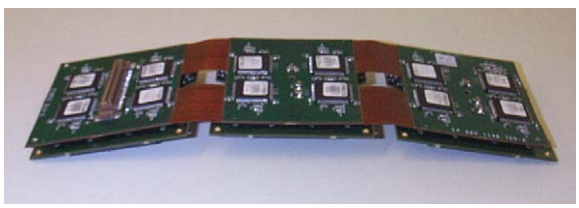

Fig. 12. TRT end-cap front-end electronics printed-circuit boards. Shown is one set of three analogue boards and one digital board, which handles 192 channels.

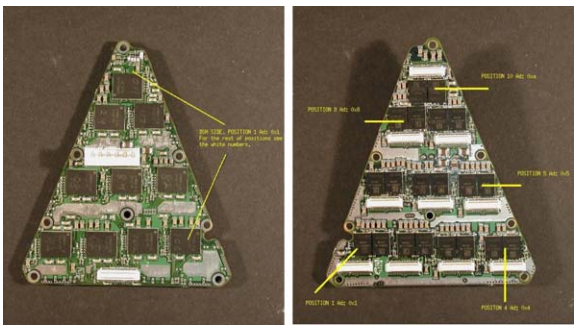

Fig. 13. TRT barrel front-end electronics printed-circuit board.

The barrel modules, on the other hand, have higher channel density, less space for the on-detector electronics and their electrical connections have a highly inhomogeneous geometry. Since the barrel straws are read out at each end to reduce occupancy, there are a total of 16 different front-end board designs to be produced in quantities of 32 each. The cooling implementation is also more complex than for the end-cap, and leaves some possibility for a fraction of the heat to reach the active gas. Other geometrical constraints have forced a design with analogue and digital chips on opposite sides of a single board as shown in Fig. 13, which has of course presented a challenge from an analogue/digital compatibility point of view. Nevertheless, prototypes produced to date have performed within specifications for most of the channels, and work is proceeding toward reliable fabrication and assembly of these complex boards.

4.4. Back-end system

The TRT back-end system, which is the interface between the on-detector electronics and the standard ATLAS Trigger, Timing and Control (TTC) and read-out (ROS) systems, is based on FPGA technology in two different 9U VME modules. The first of these, called read-out driver (ROD), receives data from the front-end electronics, performs data compression and sends the data to the ROS. The second module, called TRT-TTC, controls three RODs, and distributes the clock and level-1 accept signals and various commands to configure the front-end electronics. Low-density prototype implementations of the two modules have provided proof-of-concept as well as a system-test platform, and full-density prototypes are currently under test for deployment in view of the TRT integration.

4.4.1. The TRT-TTC module

The TRT-TTC receives clock signals, level-1 accepts and trigger information from the ATLAS TTC system. Clocks and level-1 accepts are fanned out to the front-end chips with adjustable timing, as described above. The TRT-TTC is also used to configure the front-end electronics and passes event-header information to its slave RODs.

4.4.2. The TRT Read-out Driver (ROD)

The TRT ROD does serial-to-parallel conversion of its 120 front-end links, performs data compression according to one of a number of possible schemes, merges chip data with TRT-TTC event-headers and sends the resulting data stream to the ATLAS data acquisition system via an on-board S-link interface. There are also provisions for local spying on full as well as compressed data using the VME-bus interface.

The raw TRT data stream would completely saturate the band-width of its read-out links at high trigger rates, so some form of data compression is clearly needed at the ROD level. Since the straw hit probability approaches 40% in some regions, naively sending the address and hit pattern of the hit straws would in fact increase the data size. The TRT data compression scheme [8] minimises the number of so-called valid straws, for which the complete drift-time information is passed on, by employing a validity gate: a straw is considered to have valid drift-time information if it has one or more discriminator bits set within a 12.5 ns validity window. The window position and width guarantee a high efficiency for straw hits produced in-time with the level-1 bunch-crossing of interest, but reduce considerably the contributions from out-of-time hits. Empty straws, invalid straws and straws with a valid drift-time measurement are encoded using variable-length words.

5. Summary

The assembly of the barrel modules in the US assembly sites has recently been completed, with a total of 105 modules built, including three spares of each type; approximately 40% of these modules have been fully tested (gain maps) before being shipped to CERN and many are currently being acceptance-tested at CERN. The assembly of the end-cap wheels is well underway in the Russian assembly sites, with approximately 70% of the wheels equipped with straws and 20% fully assembled. About 10% of the 8-plane wheels have been fully acceptance tested (including gain maps) at CERN and are found to be within specifications.

The on-detector front-end electronics is in production. The TRT front-end integrated circuits have been demonstrated to fulfill the requirements in terms of operation, performance and radiation hardness, and have all been manufactured over the last year. The front-end boards are in their final prototyping stages and will be manufactured over the next months. The back-end module prototypes are well beyond proof-of-concept and have been extensively used in system tests and test-beam measurements.

The detector modules and front-end electronics boards will be integrated together over the next year, the barrel and end-cap TRT parts will be assembled and tested with their SCT counterparts during 2005 and installation and commissioning in the ATLAS pit will take place at the end of 2005 and the beginning of 2006.

References

[1] ATLAS Collaboration, ATLAS inner detector technical design report, CERN/LHCC/97-17, 2, 1997.
[2] T. Akesson, et al., Nucl. Instr. and Meth. A 507 (2003) 622.
[3] V. Tikhomirov et al., ATLAS transition radiation test-beam results, Nucl. Instr. and Meth. A, (2004) these Proceedings.
[4] A. Romaniouk et al., Operation of the ATLAS transition radiation tracker under very high irradiation at the CERN LHC, Nucl. Instr. and Meth. A, (2004) these Proceedings.
[5] J. Valls, A. Romaniouk, Irradiation tests with an 8-plane TRT end-cap sector prototype. ATLAS Internal Note ATL-INDET-2002-018, 2002.
[6] J. Valls, A. Romaniouk, High rate photon irradiation test, ATLAS internal note, ATL-INDET-2002-019, 2002.
[7] M.S. Passmore, et al., Efficiency and High-Rate Performance of the TRT, ATLAS Internal Note, ATL-INDET-2003-002, 2003.
[8] M. Dam, A study of ROD compression schemes for the TRT, ATLAS Internal Note, ATL-INDET-2001-019, 2001.